Research Article

A multi-channel collagen scaffold loaded with neural stem cells for the repair of spinal cord injury

https://doi.org/10.4103/1673-5374.310698
Date of submission: September 26, 2020
Date of decision: November 3, 2020
Date of acceptance: January 29, 2021
Date of web publication: March 25, 2021

Shuo Liu[1, #], Yuan-Yuan Xie[1, #], Liu-Di Wang[1], Chen-Xu Tai[1], Dong Chen[1], Dan Mu[2], Yan-Yan Cui[3], Bin Wang[1, *]

Graphical Abstract *Collagen scaffold with neural stem cells (NSCs) facilitates the spinal cord regeneration*

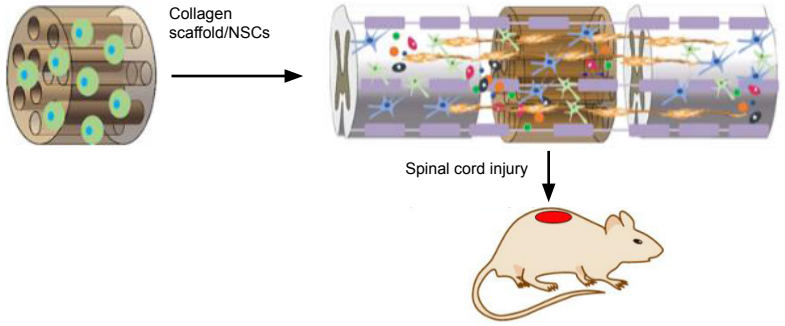

Abstract

Collagen scaffolds possess a three-dimensional porous structure that provides sufficient space for cell growth and proliferation, the passage of nutrients and oxygen, and the discharge of metabolites. In this study, a porous collagen scaffold with axially-aligned luminal conduits was prepared. *In vitro* biocompatibility analysis of the collagen scaffold revealed that it enhances the activity of neural stem cells and promotes cell extension, without affecting cell differentiation. The collagen scaffold loaded with neural stem cells improved the hindlimb motor function in the rat model of T8 complete transection and promoted nerve regeneration. The collagen scaffold was completely degraded *in vivo* within 5 weeks of implantation, exhibiting good biodegradability. Rectal temperature, C-reactive protein expression and CD68 staining demonstrated that rats with spinal cord injury that underwent implantation of the collagen scaffold had no notable inflammatory reaction. These findings suggest that this novel collagen scaffold is a good carrier for neural stem cell transplantation, thereby enhancing spinal cord repair following injury. This study was approved by the Animal Ethics Committee of Nanjing Drum Tower Hospital (the Affiliated Hospital of Nanjing University Medical School), China (approval No. 2019AE02005) on June 15, 2019.

Key Words: axially-aligned luminal conduits; biomaterial; cell transplantation; collagen; complete transection; inflammation; neural stem cell; regeneration scaffold; spinal cord injury; tissue engineering

Chinese Library Classification No. R456; R744; R318.08

Introduction

Spinal cord injury (SCI) is a severe traumatic injury that can lead to permanent nerve damage and volitional movement deficits. Currently, clinical treatment of SCI is largely ineffective (Saruhashi et al., 1996). A series of complex pathological processes result in a microenvironment that is inhibitory to neuronal regeneration after SCI, including glial scar formation, neuronal damage and loss, massive inflammatory cell infiltration, and other adverse events (Mukhamedshina et al., 2019). Reconstructing the microenvironment for nerve regeneration is a challenge for the effective treatment of SCI (Fan et al., 2017). Recently, neural stem cells (NSCs) have been widely used in SCI research as seeding cells because of their potential for replacing the injured spinal cord tissue by proliferation and differentiation and/or providing nutritional support for repair (Cummings et al., 2005; Mothe and Tator, 2013; Li et al., 2016). Some studies suggest that the newly differentiated neurons can participate in neural transmission and convey the activity of surviving host axons above and below the damaged segments, thereby improving motor

[1]Clinical Stem Cell Center, Nanjing Drum Tower Hospital, the Affiliated Hospital of Nanjing University Medical School, Nanjing, Jiangsu Province, China;
[2]Department of Radiology, Nanjing Drum Tower Hospital, the Affiliated Hospital of Nanjing University Medical School, Nanjing, Jiangsu Province, China;
[3]Department of Cell Biology and Genetics, Chongqing Medical University, Chongqing, China
***Correspondence to:** Bin Wang, PhD, wangbin022800@126.com.
https://orcid.org/0000-0003-3981-8849 (Bin Wang)
#Both authors contributed equally to this work.

Funding: *The study was supported by the National Key Research and Development Program of China, No. 2017YFA0104304 (to NG); the National Natural Science Foundation of China, Nos. 81571213 (to BW), 81800583 (to YYX), 81601539 (to DM); the Nanjing Medical Science and Technique Development Foundation of China, Nos. QRX17006 (to BW), QRX17057 (to DM); the Key Project Supported by Medical Science and Technology Development Foundation, Nanjing Department of Health and the Nanjing Medical Science and Innovation Platform of China, No. ZDX16005 (to BW); and Chongqing Yuzhong District Science and Technology Commission Project of China, No. 20140112 (to YYC).*
How to cite this article: *Liu S, Xie YY, Wang LD, Tai CX, Chen D, Mu D, Cui YY, Wang B (2021) A multi-channel collagen scaffold loaded with neural stem cells for the repair of spinal cord injury. Neural Regen Res 16(11):2284-2292.*

function (Lu et al., 2012, 2014, 2017; Kadoya et al., 2016). However, transplanted NSCs often spread to the surrounding undamaged spinal cord tissue and scarcely remain in the injured area, diminishing therapeutic effectiveness.

Biomaterial scaffolds play a key role in constructing a microenvironment conducive to regeneration in SCI repair. For example, biomaterial scaffolds can be used not only as a supporting platform to bridge the defect in SCI, but also as a carrier of seed cells to reconstruct the microenvironment at the SCI site (Xu et al., 2017). Cells can be packaged into biomaterial scaffolds to control the diffusion rate after implantation (Ogawa et al., 2002; Rooney et al., 2011; McCreedy et al., 2014). At present, the biomaterials used for cell scaffolds in SCI are commonly classified into natural and synthetic materials. Natural materials include collagen, chitosan, gelatin, sodium alginate, hyaluronic acid, and others, which have good biocompatibility and biodegradability, low immunogenicity, and favorable cell adsorption (Libro et al., 2017). Collagen protein is abundant in the extracellular matrix and is highly conserved among species. Collagen scaffold is one of the most commonly used natural biomaterials for the treatment of SCI (Yoshii et al., 2004) because of its advantageous characteristics that promote the adhesion, proliferation, differentiation, and migration of seed cells (Guan et al., 2013; Murphy et al., 2017).

The biomaterial scaffolds need a three-dimensional porous structure to provide enough space for the growth and proliferation of cells, to accommodate the flux of nutrients and oxygen, and discharge metabolites (Nomura et al., 2006; Lee et al., 2009). In this study, to facilitate the loading of NSCs, we designed a collagen scaffold with axially-aligned luminal conduits for SCI repair. The porous collagen scaffold loaded with NSCs was transplanted into the completely-transected rat spinal cord, and we evaluated behavioral recovery, axonal regeneration, biomaterial degradation, and infiltration of immune cells in these animals.

Materials and Methods

Preparation of collagen scaffolds

Collagen scaffolds were prepared by freeze-drying (Chen et al., 2018). Briefly collagen from bovine aponeurosis (Yantai Zhenghai Bio-tech Co., Ltd., Yantai, China) was dissolved in acetic acid (0.5 M) for 10 hours at 4°C, homogenized for 20 minutes, and neutralized with NaOH (4 M). The homogenate was dialyzed for 4 days and then transferred into a mold to form a porous collagen scaffold with axially-aligned luminal conduits by freeze-drying. The scaffolds were sterilized by 60Co before cell seeding.

Mechanical tests were carried out with an Instron 5943 single column testing machine (Instron, Norwood, MA, USA) to check the compressive resistance of the scaffolds. In the vertical direction, pressure was applied to the scaffold at a speed of 0.01 mm/s to produce 50% deformation, and then removed. This procedure assessed the effect of compressive stress on the scaffold and was repeated 10 times to determine compressive capacity.

The porosity of scaffolds was measured with the following method. An appropriate pycnometer (WEISS, Jiaxing, China) was filled with ethanol. The weight was W_1. The collagen scaffold was placed into the ethanol after weighing (W_s). We ensured that the ethanol filled the pores of the porous collagen scaffold. The weight was W_2. After taking out the scaffold, the weight of the ethanol and pycnometer was W_3.

Volume of collagen scaffold:

$$V_s = (W_1 - W_2 + W_s)/\rho\text{ethanol} \quad (1)$$

Pore volume of collagen scaffold:

$$V_p = (W_2 - W_3 - W_s)/\rho\text{ethanol} \quad (2)$$

Porosity of collagen scaffold:

$$\varepsilon = V_p/(V_p + V_s) \times 100\% \quad (3)$$

Culture and labeling of NSCs

Pregnant rats were anesthetized with isoflurane (RWD, Shenzhen, China). Hippocampi were dissected from 10 Sprague-Dawley rat embryos (embryonic day 12–14, specific pathogen free, provided by the Laboratory Animal Center of Nanjing Medical University (license No. SYXK (Su) 2014-0052)) and digested in accutase at 37°C for 20 minutes. The tissue was washed twice with phosphate-buffered saline (PBS) and then pipetted into a single-cell suspension in serum-free Dulbecco's modified Eagle medium/Nutrient Mixture F-12 (DMEM/F12) medium (Gibco, Grand Island, NY, USA). After filtering through a 40 μm cell sieve, the cell suspension was cultured in a 25 cm^2 tissue culture flask (Corning, Steuben County, NY, USA) with serum-free DMEM/F12 medium containing 20 ng/mL epidermal growth factor (Peprotech Asia, Rehovot, Israel), 20 ng/mL basic fibroblast growth factor (Peprotech Asia), 2% B27 (Gibco, Grand Island, NY, USA), and 1% penicillin-streptomycin (Gibco). After 4 days in culture, neurospheres were digested into single cells and resuspended in complete DMEM/F12 medium containing 10% fetal bovine serum. A total of 3×10^5 cells were seeded on a cell slide and collagen scaffolds in a 12-well plate. The medium was removed after 1 day of culture and differentiation medium (DMEM/F12 containing 2% B27) was added to induce the differentiation of NSCs.

Neurosphere of NSCs derived from rat fetal hippocampus was digested into single cells with accutase and then seeded on a cell slide and collagen scaffolds. Calcein-AM/propidium iodide (PI) double staining was performed to investigate the survival of NSCs on the collagen scaffolds. Briefly, 100 μL staining working solution (calcein-AM at 2 μM and PI at 4.5 μM) was mixed with 200 μL cell suspension and cultured at 37°C for 15 minutes. Images were taken under the Leica DMi8 Confocal Microscope (Leica Microsystems, Wetzlar, Germany).

To observe the growth of NSCs in the conduit structure of the scaffolds, we used the living cell marker CM-Dil (Gibco) to label the NSCs. Neurospheres were digested into single cells and incubated with CM-Dil (20 μg/mL) at 37°C for 15 minutes and then 4°C for 15 minutes. After centrifugation, the cells were washed with PBS and then seeded on scaffolds. Differentiation culture was performed as described above. Cells were observed on a Leica DMi8 confocal microscope (Leica Microsystems).

Scanning electron microscopy

After 5 days of culture in differentiation medium, NSCs seeded on the collagen scaffolds were fixed in 2% glutaraldehyde for 40 minutes at 4°C, followed by dehydration through a graded ethanol series (20%, 40%, 60%, 80%, 90% and 95% for 10 minutes each, and then 100% for 20 minutes). Thereafter, the collagen scaffolds were coated with gold by sputtering. Images were taken on a JEM-200CX scanning electron microscope (SEM; JEOL, Tokyo, Japan).

Surgical procedure for SCI

All animal experiments were performed in accordance with the Guide for the Care and Use of Laboratory Animals of the National Institutes of Health. This study was approved by the Animal Ethics Committee of Nanjing Drum Tower Hospital (the Affiliated Hospital of Nanjing University Medical School), China (approval No. 2019AE02005) on June 15, 2019. The record card number of professional skill training of experimental animals in Jiangsu province is 220170983.

A total of 48 adult female Sprague-Dawley rats (200–250 g,

specific pathogen free, provided by the Laboratory Animal Center of Nanjing Medical University (license No. SYXK (Su) 2014-0052)) were housed in temperature and humidity-controlled animal dormitories with a light/dark cycle of 12/12 hours for 10 days. All experimental rats were randomly allocated into the SCI group without any treatment, collagen scaffold group (SCI + collagen scaffold) or the NSCs/collagen scaffold group (SCI + NSCs/collagen scaffold) (n = 16 rats/group).

All rats were anesthetized with isoflurane. A 2-cm midline incision was made to expose the T7–9 vertebrae, and a 3-mm segment of the T8–9 spinal cord was completely transected with eye scissors. An approximately 3-mm-long piece of collagen scaffold with axially-aligned luminal conduits alone or loaded with NSCs (1×10^6 cell) was transplanted into the spinal cord defect, and the muscle tissue and skin were sewn. The animals were returned to their cage after recovery from anesthesia. After operation, rats were injected with antibiotics (Yuekang, Beijing, China) and glucose (DaZhong, Tianjin, China) for 5 days. Due to the abnormal micturition reflex, each rat was micturated manually every day and was given routine post-operative care each day.

Histological analysis

Rats were sacrificed at 1, 3, 5 and 8 weeks after surgery. All rats were anesthetized by subcutaneous injection of ketamine at 40 mg/kg and atropine sulfate at 0.05 mg/kg, and then perfused with PBS and 4% paraformaldehyde in PBS. Spinal cords were dissected, post-fixed for 48 hours at 4°C, and transferred to 20% sucrose (48 hours at 4°C) and then 30% sucrose (72 hours at 4°C). The segments were then embedded in paraffin and cut into 5-μm-thick sections on a Leica RM2235 (Leica Biosystems). Adjacent tissue sections were stained with hematoxylin and eosin for general observation of cellular and extracellular matrix features, and Masson's trichrome (Cat# BA4079A; BASO, Zhuhai, China) staining was used to observe the degradation of the collagen scaffold *in vivo*. Briefly, after the frozen section was fixed, it was stained with hematoxylin and eosin, then washed with water, dehydrated through a graded alcohol series, and cleared with xylene and sealed with neutral resin. For immunofluorescence staining, primary antibodies were applied to the sections and incubated overnight at 4°C. The primary antibodies were the following: β-tubulin (Tuj-1; 1:500; mouse; Cat# ab7751; Abcam, Cambridge, UK), neurofilament (NF; 1:200; mouse; Cat# ab3966; Abcam), glial fibrillary acidic protein (GFAP; 1:500; rabbit; Cat# ab7260; Abcam), 5-hydroxytryptamine (5-HT; 1:300; rabbit; Cat# 20080; Immunostar, Hudson, WI, USA), CD68 (1:400; mouse; Cat# 36-1965; Abeomics, Inc., San Diego, CA, USA), and CD206 (1:400; rabbit; Cat# 18704-1-AP; Proteintech, Wuhan, China). Sections were then incubated with secondary antibody (Alexa Fluor 488 donkey anti-mouse, Cat# A21202; Alexa Fluor 488 goat anti-rabbit, Cat# A11034, 1:500; Alexa Fluor 568 goat anti-rabbit, Cat# A11011; Alexa Fluor 568 goat anti-mouse, Cat# A11031; all 1:500; provided by Invitrogen, Carlsbad, CA, USA) for 1 hour at room temperature. Cell nuclei were stained with 4′,6-diamidino-2-phenylindole (DAPI; Cat# ab104139; Abcam) and images were taken under the Leica DMi8 confocal microscope.

Inflammatory reaction

The inflammatory reaction is a double-edged sword for SCI repair. We examined whether the collagen scaffold and NSC transplant elicit adverse inflammatory responses. Here, we monitored various indicators of inflammation, including rectal temperature, C-reactive protein (CRP), CD68 (a marker of macrophages (Chedly et al., 2017)) and CD206 (a marker of M2 macrophages (Chedly et al., 2017)). Blood samples were collected from the inner canthus at 0, 1, 3, 5 and 7 days after surgery, and the sera were stored at –80°C for CRP enzyme-linked immunosorbent assay analysis.

Behavioral assessment

The hindlimb motor function of all experimental rats was assessed with the Basso, Beattie and Bresnahan (BBB) locomotor rating scale (Basso et al., 1996). The BBB scale scores range from 0 (complete paralysis) to 21 points (normal motor function). The BBB test was performed by two independent observers blinded to the treatments, and hindlimb function was scored when the rats moved freely in an open field every week after operation. The assessment was performed for 5 minutes. Rats were allowed to move freely based on their spontaneous hind limb movement. A detailed scoring procedure is provided in **Additional Table 1** (Basso et al., 1996).

Statistical analysis

GraphPad Prism version 6.0 (GraphPad Software, San Diego, CA, USA) was used to estimate significance and produce graphs. The data are presented as mean ± standard derivation (SD) from a minimum. A one-way analysis of variance was performed followed by Tukey's *post hoc* test for pairwise comparison if the data were normally distributed. A P-value < 0.05 indicated statistical significance. Three replicates were done for each experiment.

Results

Characteristics of collagen scaffold with axially-aligned luminal conduits

The collagen scaffold with axially-aligned luminal conduits was fabricated as a cylindrical scaffold of 3-mm diameter and 3-mm thickness, with axially-aligned luminal conduits for directional axonal growth and promoting connections between distal and proximal axons (**Figure 1A** and **B**). SEM images showed this collagen scaffold had uniform sponge-like pores, suggesting that it should provide enough space for the adhesion and growth of seeded cells (**Figure 1C** and **D**). **Figure 1E** shows a sketch of the mold for preparing the collagen scaffold with axially-aligned luminal conduits.

The mechanical properties of the scaffold are shown in **Figure 1F** and **G**. The compressive strength of the scaffold was 107.73–233 kPa (**Figure 1F**). After 10 compression cycles, the collagen scaffold could partially maintain its structure (**Figure 1G**). Thus, the scaffold should have sufficient mechanical strength for transplantation.

To meet the requirements of tissue engineering, the porosity of the scaffolds must usually be higher than 80%. The porosity of the collagen scaffold with axially-aligned luminal conduits is shown in **Additional Table 2**. The scaffolds satisfy this requirement.

Biocompatibility of NSCs on collagen scaffold with axially-aligned luminal conduits

Calcein-AM/PI double staining showed that NSCs had good adhesion and growth on the collagen scaffolds (**Figure 2A**), which was confirmed by SEM analysis (**Figure 2B**). The data indicate that the NSCs on the collagen scaffolds had a similar viability at 3 days, but a markedly higher viability at 5 days, compared with NSCs on cell slides (**Figure 2C**). The growth and differentiation of NSCs in the conduit structure of the scaffold is shown in **Figure 2D**. The cells grew linearly along the conduit structure, which helps to connect the damaged nerves and promote recovery following SCI. The differentiation of NSCs on the collagen scaffolds was investigated using immunostaining for Tuj-1, a neuronal marker, and GFAP, an astrocyte marker (**Figure 2E**). The collagen scaffolds supported the differentiation of NSCs and the neuronal and astrocytic differentiation of NSCs, similar to NSCs in normal two-dimensional culture (**Figure 2F** and **G**). These results indicate that our collagen scaffold has very good biocompatibility and is suitable for adhesion, growth and differentiation of NSCs *in vitro*.

Transplantation of collagen scaffolds loaded with NSCs promotes locomotor functional recovery in the rat model of SCI

NSCs were loaded into axially-aligned luminal conduits of collagen scaffolds and transplanted into the defect of the completely-transected T8 spinal cord (**Figure 3A** and **B**). The recovery of locomotor function is the most important indicator and goal of SCI therapy (Li et al., 2017). The BBB score of all rats was 21 before operation. The hindlimbs of rats were completely paralyzed immediately after SCI, with a BBB score of 0. The rats in the SCI group had very limited locomotor recovery of the hindlimbs, with BBB scores of 2–3 at 8 weeks post-surgery (**Figure 3C**). Collagen scaffold transplant only increased slightly the BBB score, about 4–5 points, at 8 weeks, without a significant difference from the SCI group. In contrast, rats with NSCs/collagen scaffold transplantation had consistent recovery in locomotor function during the observation period, with a significantly higher BBB score (about 7–8 points at 8 weeks) compared with the SCI and collagen scaffold alone groups ($P < 0.05$; **Figure 3C**). These results indicate that the collagen scaffold loaded with NSCs in axially-aligned luminal conduits markedly promotes the recovery of locomotor function in paraplegic rats after complete-transection SCI.

Transplantation of collagen scaffolds loaded with NSCs improves the injured spinal cord tissue structure and collagen degradation in SCI rats

Functional recovery is attributed to changes in tissue structure and pathophysiology (Fan et al., 2018). Hematoxylin and eosin staining was used to observe structural changes in the injured spinal cord at the indicated time points (**Figure 4A**). In the SCI group, the tissue at the site of injury showed a loose and disordered structure, accompanied with cavities of uneven size. In contrast, the collagen scaffold and NSCs/collagen scaffold groups both had compact tissues at the lesion site, and no obvious cavity was observed. The structure of the lesion/scaffold site can be seen clearly in high-power images (**Figure 4B**). The degradation of collagen scaffold transplants in SCI repair is a major concern (Sun et al., 2019), thus Masson staining was performed to investigate the collagen deposits at the site of injury after transplantation at different time points (**Figure 4C**). At 1 week, Masson staining was very intense both in the collagen scaffold and NSCs/collagen scaffold groups, indicating collagen was mostly undegraded at the lesion site. At 3 weeks, the intensity of the blue faded, and the blue-stained area markedly decreased in the collagen scaffold and NSCs/collagen scaffold groups, suggesting the transplanted collagen scaffolds had dramatically degraded in the injured spinal cord. Notably, at 5 and 8 weeks, Masson staining was very weak in the collagen scaffold and NSCs/collagen scaffold groups. These results indicate that our collagen scaffold had a good degradation rate *in vivo* and was almost completely degraded within 5 weeks after transplantation.

Transplantation of collagen scaffolds loaded with NSCs improves nerve regeneration in SCI rats

Recent studies suggest that newly differentiated neurons derived from endogenous or exogenous NSCs formed a relay to transmit the activity of surviving damaged host axons above and below the injury levels (Lu et al., 2012; Lai et al., 2016). Immunofluorescence staining of longitudinal sections showed that the collagen scaffold group had more Tuj-1-positive cells in the injured spinal cord than the SCI group ($P < 0.01$), while the NSCs/collagen scaffold group had much more Tuj-1-positive cells than the collagen scaffold and SCI groups ($P < 0.001$; **Figure 5A** and **B**). In contrast, hypertrophic GFAP-positive astrocytes were observed in the SCI and collagen scaffold groups, while the NSCs/collagen scaffold group had a notable decrease in reactive astrogliosis (**Figure 5A** and **C**).

It is crucial for regenerating axons to transmit neural signals across the injured spinal cord segment. 5-HT nerve fibers participate in the activity of the spinal cord neural network involved in vertebrate movement after SCI (Liu et al., 2019). Here, immunostaining for NF and 5-HT was used to assess axon regeneration (**Figure 5D–F**). NF immunoreactivity was distributed throughout the lesion site in the three groups at 8 weeks after surgery. Quantitative analysis showed that the collagen scaffold group had more NF-positive axons than the control group ($P < 0.01$; **Figure 5E**). The NSCs/collagen scaffold group had more NF-positive axons compared with the collagen scaffold and SCI groups (**Figure 5E**). Similar to NF staining, the NSCs/collagen scaffold group had more 5-HT-positive axons than the collagen scaffold and SCI groups ($P < 0.001$). In addition, 5-TH staining was heavier in the collagen scaffold group compared with the SCI group ($P < 0.01$; **Figure 5F**).

Transplantation of collagen scaffolds loaded with NSCs decreases inflammation in SCI rats

The normal rectal temperature was 38.57 ± 0.49°C in rats, but was markedly lower in all rats after surgery. Consecutive rectal temperature monitoring showed that there was no statistical difference among the three groups at the indicated time points (**Figure 6A**). The serum CRP concentration was 758.71 ± 174.5 ng/mL before surgery, and was markedly increased to 1,349.56 ± 451.41 ng/mL at day 1 post-surgery, and then quickly returned to normal levels in the SCI group. The scaffold and NSCs/scaffold transplant groups did not show changes in CRP levels at the indicated times, other than day 5 post-surgery, and the NSCs/collagen scaffold group had a higher CRP level than the collagen scaffold group ($P < 0.05$; **Figure 6B**). To investigate macrophage infiltration at the lesion site, immunostaining for CD68 and CD206 was performed at 1, 4 and 8 weeks after surgery. Evident positive staining for CD68 and CD206 was observed among the three groups at all time points (**Figure 6C–E**). There were more CD68-positive macrophages in the NSCs/collagen scaffold group, compared with the SCI group at 1 week post-surgery. We noticed that the CD68-positive cells in the collagen scaffold and NSCs/collagen scaffold groups had an appearance distinct from those in the SCI group, which exhibited a round morphology. CD206 is a marker of M2 macrophages, which are considered to play an anti-inflammatory role in SCI repair (Chedly et al., 2017). CD206 staining showed that the scaffold and NSCs/scaffold transplants increased M2 macrophage infiltration into the lesion site at 8 weeks after SCI (**Figure 6C–E**). These results clearly indicate that our collagen scaffold has low immunogenicity and does not elicit an obvious adverse inflammatory response following SCI.

Discussion

Currently, SCI repair remains a major challenge, and there is still no effective clinical treatment. Here, we designed a novel porous collagen scaffold with axially-aligned luminal conduits as a nerve regenerative material for SCI repair. This scaffold had very good biocompatibility for NSCs *in vitro* such as good adhesion and neural differentiation. The collagen scaffold loaded with NSCs in axially-aligned luminal conduits was transplanted into the completely-transected spinal cord at the T8 level in rats, and evident therapeutic effects were observed. The scaffold loaded with NSCs markedly improved locomotor functional recovery and nerve regeneration compared with the SCI and collagen scaffold groups. In addition, our collagen scaffold had good degradation and low immunogenicity. The transplanted scaffold completely degraded within 5 weeks and did not induce adverse inflammatory responses such as abnormal rectal temperature, CRP or CD68-positive immune cell infiltration.

The loss of neurons caused by SCI destroys the ascending and descending fibers of the spinal cord, which leads to the successive dysfunction of sensory and motor functions below the injury site (Bradbury and McMahon, 2006; Thuret et al.,

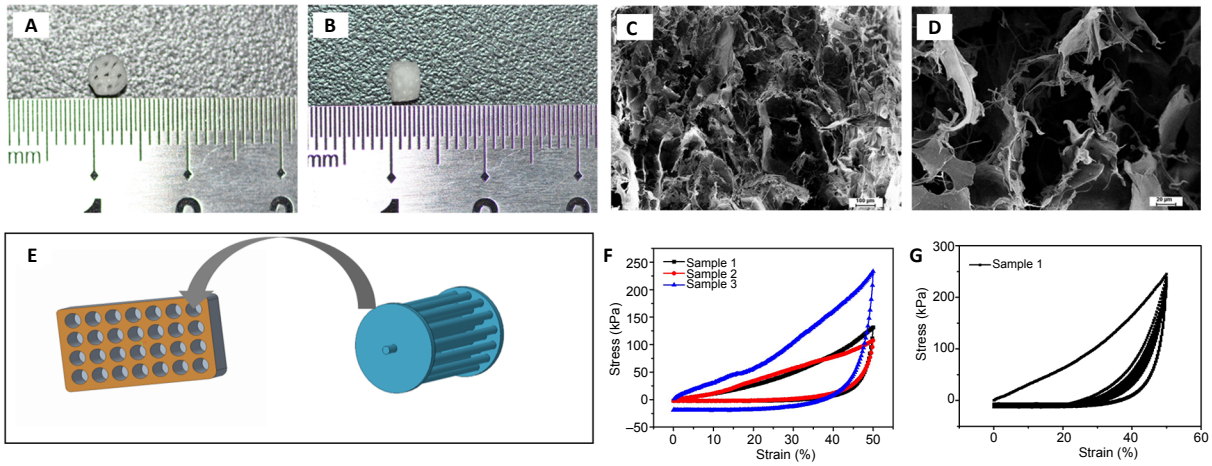

Figure 1 | **Characterization of the collagen scaffold with axially-aligned luminal conduits.**
(A, B) The collagen scaffold with a 3-mm diameter and 3-mm thickness, containing axially-aligned luminal conduits. (C, D) Scanning electron microscopy image showing the porous morphology of the collagen scaffold. Scale bars: 100 μm in C, 20 μm in D. (E) Schematic diagram of the mold for preparing the scaffold. (F, G) The compressive capacity of the collagen scaffold.

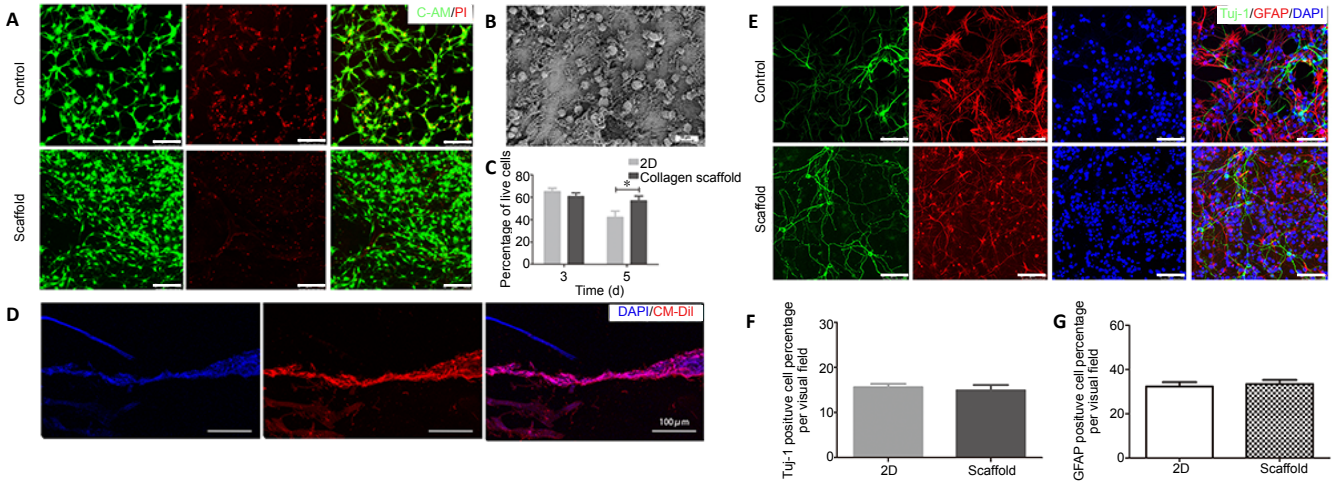

Figure 2 | **Biocompatibility of the collagen scaffold with axially-aligned luminal conduits.**
(A) Confocal images of C-AM/PI double staining at 5 days. Live cells are labeled green and red signals indicate dead cells. Compared with the control group, NSCs inoculated on the scaffold had a better survival rate. (B) Scanning electron microscopy image of NSCs cultured on the collagen scaffold for 5 days. (C) The quantification of living NSCs. (D) Good growth of CM-DiI-labeled NSCs in the conduit structure of scaffolds. (E) Representative images of immunostaining for Tuj-1 (neurons, Alexa Fluor 488, green) and GFAP (astrocytes, Alexa Fluor 568, red). NSCs inoculated on the scaffolds could differentiate normally as in the control group. (F, G) The quantification of Tuj-1 and GFAP-positive cells in a 200× field. Scale bars: 100 μm. Data are presented as mean ± SD. The experiment was repeated three times. *$P < 0.05$ (one-way analysis of variance followed by Tukey's *post hoc* test). 2D: Two-dimensional; C-AM: Calcein-AM; DAPI: 4′,6-diamidino-2-phenylindole; GFAP: glial fibrillary acidic protein; NSCs: neural stem cells; PI: propidium iodide; Tuj-1: βIII-tubulin.

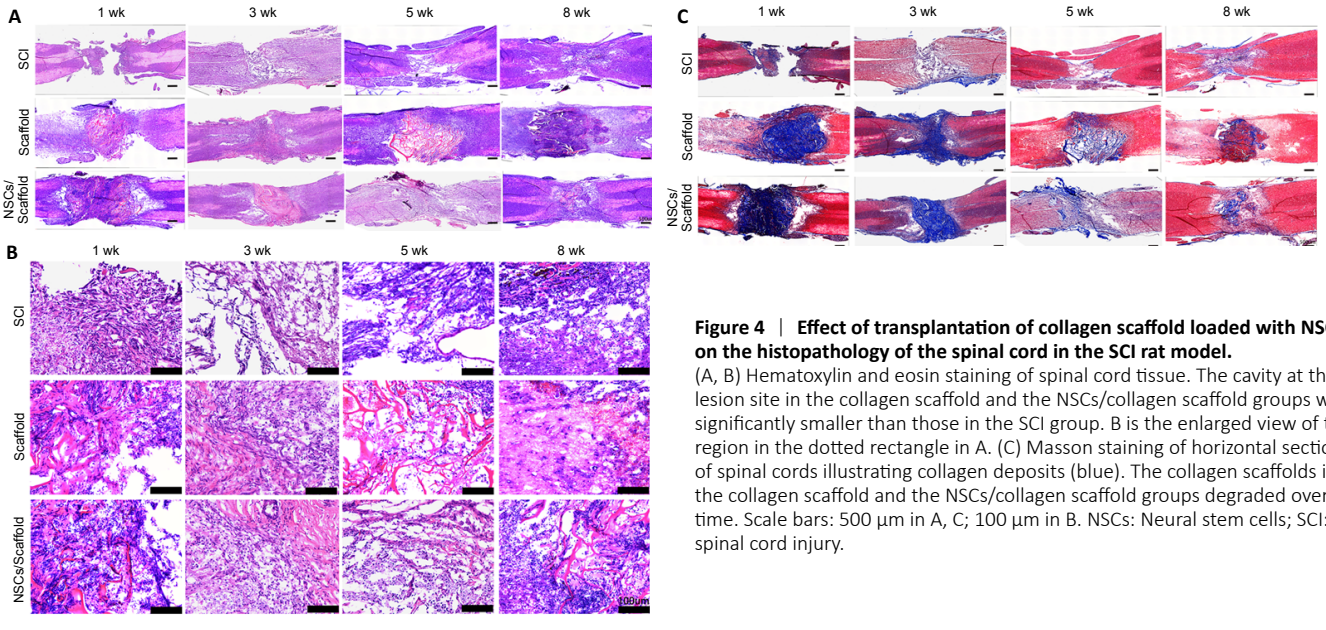

Figure 4 | **Effect of transplantation of collagen scaffold loaded with NSCs on the histopathology of the spinal cord in the SCI rat model.**
(A, B) Hematoxylin and eosin staining of spinal cord tissue. The cavity at the lesion site in the collagen scaffold and the NSCs/collagen scaffold groups were significantly smaller than those in the SCI group. B is the enlarged view of the region in the dotted rectangle in A. (C) Masson staining of horizontal sections of spinal cords illustrating collagen deposits (blue). The collagen scaffolds in the collagen scaffold and the NSCs/collagen scaffold groups degraded over time. Scale bars: 500 μm in A, C; 100 μm in B. NSCs: Neural stem cells; SCI: spinal cord injury.

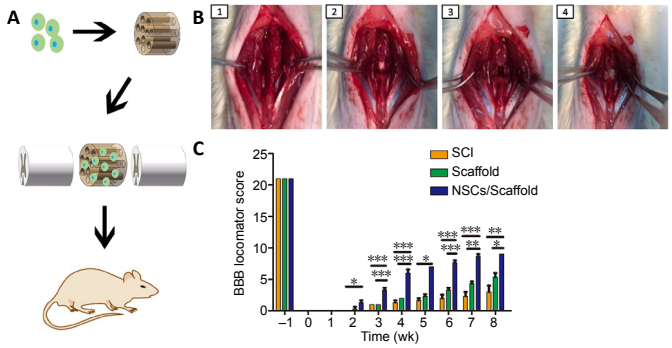

Figure 3 | Effect of transplantation of collagen scaffolds loaded with NSCs on motor functional recovery in SCI model rats.
(A) Schematic diagram of the experimental protocol. (B) SCI surgery at T8–9 spinal cord and treatment. 1–4 show the procedure of the operation. (C) The BBB score analysis during the observation period. Data are presented as mean ± SD (n = 16). *P < 0.05, **P < 0.01, ***P < 0.001 (one-way analysis of variance followed by Tukey's *post hoc* test). BBB: Basso, Beattie and Bresnahan; NSCs: neural stem cells; SCI: spinal cord injury.

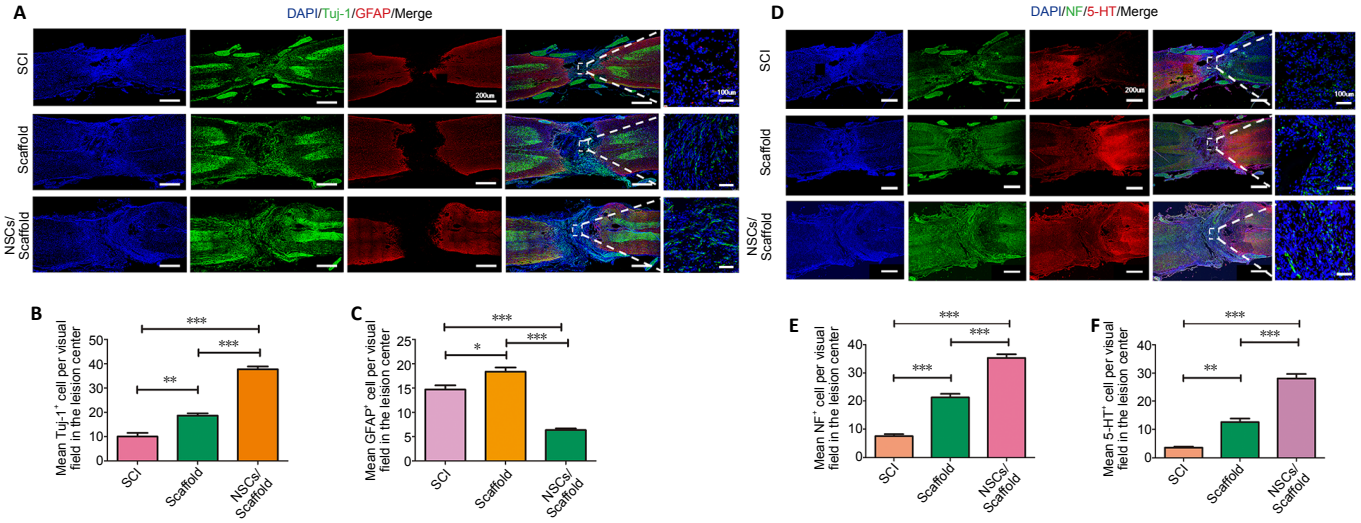

Figure 5 | NSCs/collagen scaffold treatment promotes nerve regeneration in SCI model rats.
(A) Immunofluorescence staining for Tuj-1 (Alexa Fluor 488, green) and GFAP (Alexa Fluor 568, red). The number of GFAP-positive astrocytes in the peri-lesional area in the SCI and collagen scaffold groups was higher than that in the NSCs/collagen scaffold group. Tuj-1-positive cells were more hypertrophic in the NSCs/collagen scaffold group compared with the SCI and collagen scaffold groups. (B, C, E, F) Quantification of Tuj-1-, GFAP-, NF- and 5-HT-positive cells in 200× field in SCI, collagen scaffold and NSCs/collagen scaffold groups. (D) Immunofluorescence staining for NF (Alexa Fluor 488, green) and 5-HT (Alexa Fluor 568, red) at the lesion site. The number of NF-positive and 5-HT-positive axons in the peri-lesional area in the NSCs/collagen scaffold group was higher than that in the other two groups. Data are presented as mean ± SD (n = 16). *P < 0.05, **P < 0.01, ***P < 0.001 (one-way analysis of variance followed by Tukey's *post hoc* test). 5-HT: 5-Hydroxytryptamine; DAPI: 4′,6-diamidino-2-phenylindole; GFAP: glial fibrillary acidic protein; NF: neurofilament; NSCs: neural stem cells; SCI: spinal cord injury; Tuj-1: βIII-tubulin.

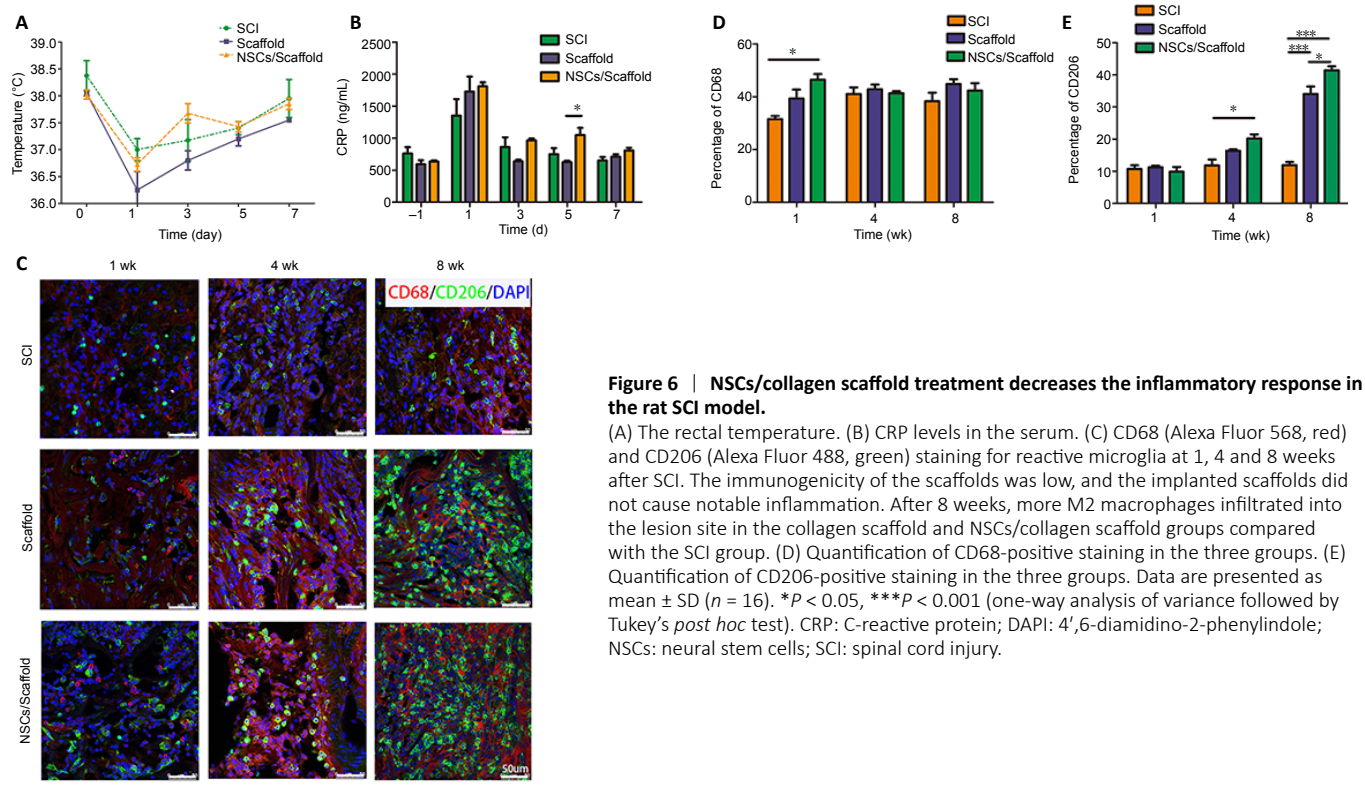

Figure 6 | NSCs/collagen scaffold treatment decreases the inflammatory response in the rat SCI model.
(A) The rectal temperature. (B) CRP levels in the serum. (C) CD68 (Alexa Fluor 568, red) and CD206 (Alexa Fluor 488, green) staining for reactive microglia at 1, 4 and 8 weeks after SCI. The immunogenicity of the scaffolds was low, and the implanted scaffolds did not cause notable inflammation. After 8 weeks, more M2 macrophages infiltrated into the lesion site in the collagen scaffold and NSCs/collagen scaffold groups compared with the SCI group. (D) Quantification of CD68-positive staining in the three groups. (E) Quantification of CD206-positive staining in the three groups. Data are presented as mean ± SD (n = 16). *P < 0.05, ***P < 0.001 (one-way analysis of variance followed by Tukey's *post hoc* test). CRP: C-reactive protein; DAPI: 4′,6-diamidino-2-phenylindole; NSCs: neural stem cells; SCI: spinal cord injury.

2006). NSCs can differentiate into many cell types, including neurons, which can promote axonal regeneration and connections, and form synaptic connections between host neurons and transplanted NSCs (Lu et al., 2012). Exogenous NSCs transplanted to sites of SCI can form a neuronal relay to transmit ascending and descending messages through the injury/graft site of the spinal cord, and promote motor functional recovery (Fan et al., 2017; Yuan et al., 2019; Jiang et al., 2020). However, treatment with NSCs alone has only a very limited therapeutic effectiveness, far from the ultimate goal of full locomotor recovery, because of various adverse factors, such as rapid cell diffusion, lack of support matrix, unfavorable niche, inflammation, and glial scar formation. Thus, tissue engineering is a promising strategy, and accumulating evidence shows that biomaterial implantation effectively contributes to nerve repair after SCI (Teng et al., 2002; Caron et al., 2016; Gomes et al., 2016). In the past few years, a variety of tissue engineering biomaterials have been used for SCI repair, such as collagen scaffolds, poly(glycolic acid) and chitosan carriers, to fill the gap in the damaged area and/or support cell adhesion. Collagen is particularly attractive in regenerative medicine and tissue engineering because of the natural abundance, inherent biological functionality, and biodegradability (Schoof et al., 2001; Deumens et al., 2010). As a cell carrier and bridging device, collagen-based scaffold material has been widely used in many experimental models of central and peripheral nervous system injuries (Altinova et al., 2019). However, the architectonics of the biomaterial scaffold has not been optimized for SCI. For example, although some biomaterial scaffolds with loaded stem cells have a three-dimensional spatial porous structure for the growth and proliferation of cells, the loaded cells only attach on the surface of the scaffold and fail to infiltrate into the interstitial space of the biomaterial, unlike the NSCs in our collagen scaffold. It has been demonstrated that the application of nerve guidance conduits can modulate the internal microenvironment by acting as a guide for the regenerating nerve ends (Cai et al., 2019). Some biomaterials have been fabricated into cell scaffolds with a channel structure (Chen et al., 2018; Jiang et al., 2020). However, given the good biocompatibility, immunogenicity and adhesivity of the material for the loaded cells, the linearly-ordered collagen scaffold has unique advantages (Liang et al., 2010; Li et al., 2018). In this study, our collagen scaffold not only possessed a porous sponge structure to accommodate enough nutrients and oxygen, and discharge metabolites, but also had axially-aligned luminal conduits to facilitate loading of the transplanted NSCs, directionally orient process extension of newly differentiated neurons, and promote connections between distal and proximal axons, resulting in increased recovery following SCI. Here, the results of *in vitro* differentiation of CM-Dil-labeled NSCs revealed that the cells could grow linearly in the conduits of the scaffolds. In addition, this design of axially-aligned luminal conduits also was conducive to the infiltration of immune cells into the core of the scaffold, which speeded up the degradation of materials and the elimination of dead cells. After verifying good biocompatibility for NSCs *in vitro*, our novel architectonic collagen scaffold loaded with NSCs in axially-aligned luminal conduits produced striking locomotor recovery, compared with the SCI and collagen scaffold groups. In addition, H&E staining revealed compact tissues in the lesion, and no obvious cavity was observed after transplantation. Immunofluorescence analysis revealed more Tuj-1, NF and 5-HT-positive cells in the injured spinal cord in rats transplanted with the collagen scaffold loaded with NSCs compared with SCI or collagen scaffold alone treatment. Axon regeneration is critical for the transmission of neural signals across the injured spinal cord, and 5-HT nerve fibers participate in the neural network activity of the spinal cord involved in vertebrate movement after SCI (Saruhashi et al., 1996; Yan et al., 2011). Our findings clearly show that the novel architectonic collagen scaffold is beneficial to the improvement of tissue structure and the regeneration of neurons in the injured area of the spinal cord, achieving, to a large extent, our primary objective of novel architectonic design for SCI repair.

A good biomaterial for SCI should have an appropriate degradation rate, synchronized with neural regeneration. Moreover, an appropriate degradation rate also accelerates axonal passage through the damaged area and prevents the formation of physical barriers (Sakiyama-Elbert et al., 2012). The degradation time of scaffolds made of some synthetic biomaterials may be several months (Koffler et al., 2019; Raynald et al., 2019), which may hinder the connection of regenerated axons and affect repair. In addition, the degradation products of some biodegradable and biocompatible synthetic scaffolds, like the poly(lactic-co-glycolic acid) scaffold, hinder the tissue-repair process (Shrestha et al., 2014). Here, we used Masson staining to investigate the degradation of our collagen scaffold *in vivo*, and found our collagen scaffold had a good degradation rate and was almost completely degraded 3–5 weeks after transplantation. BBB scoring showed that locomotor functional recovery was markedly improved 3–5 weeks post-surgery, indicating the degradation of the transplanted collagen scaffold was synchronized with neural regeneration. The degradation of the scaffold provides space for nerve regeneration, which is beneficial to the repair of SCI. We were concerned that our collagen scaffold transplant might elicit adverse inflammatory responses. Body temperature and CRP are important indicators of inflammation after injury. In this study, there were no changes in rectal temperature or serum CRP levels after transplantation of the collagen scaffold alone or the scaffold seeded with NSCs, compared with rats given no treatment. We further investigated immune cell infiltration at the lesion site, and found that the collagen scaffold alone or scaffold loaded with NSCs did not increase the infiltration of CD68-positive cells. CD68 is a surface marker of macrophages, microglia, monocytes and granulocytes (Saito et al., 1991; Bolós et al., 2019; Wang et al., 2019). These results indicate that our collagen scaffold has low immunogenicity and does not induce an adverse inflammatory response.

There are some limitations to this study. Here, we found that transplantation of the collagen scaffold alone did not markedly improve locomotor functional recovery. Locomotor functional recovery in complete-transection SCI is affected by multiple factors. The remyelination of regenerating axons is a key factor, and enhancing the differentiation of NSCs after transplant is a challenge. Adequate neurotrophic factor support is crucial for neural functional recovery (Han et al., 2019). The cooperative interaction of basic fibroblast growth factor and the collagen scaffold can enhance the proliferation and viability of the seeded NSCs (Li et al., 2016). In future experiments, we will consider adding nutritional factors or other methods to improve repair after SCI. Endogenous NSCs appear to be present in many regions of the adult spinal cord (Gage, 2000; Barnabé-Heider et al., 2010; Luo et al., 2015). The scaffolds with aligned nanofibers or parallel microchannels are more beneficial for guiding nerve regeneration and extension, promoting neuronal differentiation of stem cells, and improving migration of endogenous NSCs (Li et al., 2018). In our current study, collagen scaffold combined with exogenous NSCs, but not the collagen scaffold alone, improved functional recovery and neural regeneration after SCI. Further study is needed to elucidate how the exogenous NSCs loaded on the scaffold contribute to locomotor functional recovery, neurogenesis and axon regeneration. Do the NSCs directly differentiate into new neurons or do they indirectly induce newborn neuronal differentiation of endogenous NSCs by secreting neurotrophic growth factors?

In summary, in this study, we engineered a novel architectonic collagen scaffold with axially-aligned luminal conduits. This scaffold is a good biomaterial for NSC loading, and exhibits therapeutic effectiveness in SCI repair, by enhancing locomotor functional recovery, neural generation and axon growth, without provoking an adverse inflammatory response.

Author contributions: *Study design and manuscript review: SL, BW; definition of intellectual content: SL, DM; experiment implementation: SL, YYX, LDW, CXT; data acquisition: SL, LDW, CXT; data analysis and manuscript preparation: SL, YYX; statistical analysis: SL, DC; manuscript editing: SL. All authors approved the final version of the manuscript.*
Conflicts of interest: *The authors declare that they have no competing interests.*
Financial support: *The study was supported by the National Key Research and Development Program of China, No. 2017YFA0104304 (to NG); the National Natural Science Foundation of China, Nos. 81571213 (to BW), 81800583 (to YYX), 81601539 (to DM); the Nanjing Medical Science and Technique Development Foundation of China, Nos. QRX17006 (to BW), QRX17057 (to DM); the Key Project Supported by Medical Science and Technology Development Foundation, Nanjing Department of Health and the Nanjing Medical Science and Innovation Platform of China, No. ZDX16005 (to BW); and Chongqing Yuzhong District Science and Technology Commission Project of China, No. 20140112 (to YYC). The funders had no roles in the study design, conduction of experiment, data collection and analysis, decision to publish, or preparation of the manuscript.*
Institutional review board statement: *This study was approved by the Animal Ethics Committee of Nanjing Drum Tower Hospital (the Affiliated Hospital of Nanjing University Medical School), China (approval No. 2019AE02005) on June 15, 2019.*
Copyright license agreement: *The Copyright License Agreement has been signed by all authors before publication.*
Data sharing statement: *Datasets analyzed during the current study are available from the corresponding author on reasonable request.*
Plagiarism check: *Checked twice by iThenticate.*
Peer review: *Externally peer reviewed.*
Open access statement: *This is an open access journal, and articles are distributed under the terms of the Creative Commons Attribution-NonCommercial-ShareAlike 4.0 License, which allows others to remix, tweak, and build upon the work non-commercially, as long as appropriate credit is given and the new creations are licensed under the identical terms.*
Open peer reviewers: *Itzhak Fischer, Drexel University College of Medicine, USA; N. Scott Litofsky, University of Missouri-Columbia School of Medicine, USA.*
Additional files:
Additional Table 1: *Basso, Beattie and Bresnahan locomotor rating scale*
Additional Table 2: *Porosity (%) of collagen scaffold with axially-aligned luminal conduits*
Additional file 1: *Open peer review reports 1 and 2.*

References

Altinova H, Hammes S, Palm M, Gerardo-Nava J, Achenbach P, Deumens R, Hermans E, Führmann T, Boecker A, van Neerven SGA, Bozkurt A, Weis J, Brook GA (2019) Fibroadhesive scarring of grafted collagen scaffolds interferes with implant-host neural tissue integration and bridging in experimental spinal cord injury. Regen Biomater 6:75-87.

Barnabé-Heider F, Göritz C, Sabelstrom H, Takebayashi H, Pfrieger FW, Meletis K, Frisén J (2010) Origin of new glial cells in intact and injured adult spinal cord. Cell Stem Cell 7:470-482.

Basso DM, Beattie MS, Bresnahan JC (1996) Graded histological and locomotor outcomes after spinal cord contusion using the NYU weight-drop device versus transection. Exp Neurol 139:244-256.

Bolós M, Terreros-Roncal J, Perea JR, Pallas-Bazarra N, Ávila J, Llorens-Martín M (2019) Maturation dynamics of the axon initial segment (AIS) of newborn dentate granule cells in young adult C57BL/6J mice. J Neurosci 39:1605-1620.

Bradbury EJ, McMahon SB (2006) Spinal cord repair strategies: why do they work? Nat Rev Neurosci 7:644-653.

Cai Z, Gan Y, Bao C, Wu W, Wang X, Zhang Z, Zhou Q, Lin Q, Yang Y, Zhu L (2019) Photosensitive hydrogel creates favorable biologic niches to promote spinal cord injury repair. Adv Healthc Mater 8:e1900013.

Caron I, Rossi F, Papa S, Aloe R, Sculco M, Mauri E, Sacchetti A, Erba E, Panini N, Parazzi V, Barilani M, Forloni G, Perale G, Lazzari L, Veglianese P (2016) A new three dimensional biomimetic hydrogel to deliver factors secreted by human mesenchymal stem cells in spinal cord injury. Biomaterials 75:135-147.

Chedly J, Soares S, Montembault A, von Boxberg Y, Veron-Ravaille M, Mouffle C, Benassy MN, Taxi J, David L, Nothias F (2017) Physical chitosan microhydrogels as scaffolds for spinal cord injury restoration and axon regeneration. Biomaterials 138:91-107.

Chen X, Zhao Y, Li X, Xiao Z, Yao Y, Chu Y, Farkas B, Romano I, Brandi F, Dai J (2018) Functional multichannel poly(propylene fumarate)-collagen scaffold with collagen-binding neurotrophic factor 3 promotes neural regeneration after transected spinal cord injury. Adv Healthc Mater 7:e1800315.

Cummings BJ, Uchida N, Tamaki SJ, Salazar DL, Hooshmand M, Summers R, Gage FH, Anderson AJ (2005) Human neural stem cells differentiate and promote locomotor recovery in spinal cord-injured mice. Proc Natl Acad Sci U S A 102:14069-14074.

Deumens R, Bozkurt A, Meek MF, Marcus MA, Joosten EA, Weis J, Brook GA (2010) Repairing injured peripheral nerves: Bridging the gap. Prog Neurobiol 92:245-276.

Fan C, Li X, Xiao Z, Zhao Y, Liang H, Wang B, Han S, Li X, Xu B, Wang N, Liu S, Xue W, Dai J (2017) A modified collagen scaffold facilitates endogenous neurogenesis for acute spinal cord injury repair. Acta Biomater 51:304-316.

Fan L, Liu C, Chen X, Zou Y, Zhou Z, Lin C, Tan G, Zhou L, Ning C, Wang Q (2018) Directing induced pluripotent stem cell derived neural stem cell fate with a three-dimensional biomimetic hydrogel for spinal cord injury repair. ACS Appl Mater Interfaces 10:17742-17755.

Gage FH (2000) Mammalian neural stem cells. Science 287:1433-1438.

Gomes ED, Mendes SS, Leite-Almeida H, Gimble JM, Tam RY, Shoichet MS, Sousa N, Silva NA, Salgado AJ (2016) Combination of a peptide-modified gellan gum hydrogel with cell therapy in a lumbar spinal cord injury animal model. Biomaterials 105:38-51.

Guan S, Zhang XL, Lin XM, Liu TQ, Ma XH, Cui ZF (2013) Chitosan/gelatin porous scaffolds containing hyaluronic acid and heparan sulfate for neural tissue engineering. J Biomater Sci Polym Ed 24:999-1014.

Han S, Yin W, Li X, Wu S, Cao Y, Tan J, Zhao Y, Hou X, Wang L, Ren C, Li J, Hu X, Mao Y, Li G, Li B, Zhang H, Han J, Chen B, Xiao Z, Jiang X, et al. (2019) Pre-clinical evaluation of CBD-NT3 modified collagen scaffolds in completely spinal cord transected non-human primates. J Neurotrauma 36:2316-2324.

Jiang JP, Liu XY, Zhao F, Zhu X, Li XY, Niu XG, Yao ZT, Dai C, Xu HY, Ma K, Chen XY, Zhang S (2020) Three-dimensional bioprinting collagen/silk fibroin scaffold combined with neural stem cells promotes nerve regeneration after spinal cord injury. Neural Regen Res 15:959-968.

Kadoya K, Lu P, Nguyen K, Lee-Kubli C, Kumamaru H, Yao L, Knackert J, Poplawski G, Dulin JN, Strobl H, Takashima Y, Biane J, Conner J, Zhang SC, Tuszynski MH (2016) Spinal cord reconstitution with homologous neural grafts enables robust corticospinal regeneration. Nat Med 22:479-487.

Koffler J, Zhu W, Qu X, Platoshyn O, Dulin JN, Brock J, Graham L, Lu P, Sakamoto J, Marsala M, Chen S, Tuszynski MH (2019) Biomimetic 3D-printed scaffolds for spinal cord injury repair. Nat Med 25:263-269.

Lai BQ, Che MT, Du BL, Zeng X, Ma YH, Feng B, Qiu XC, Zhang K, Liu S, Shen HY, Wu JL, Ling EA, Zeng YS (2016) Transplantation of tissue engineering neural network and formation of neuronal relay into the transected rat spinal cord. Biomaterials 109:40-54.

Lee SH, Chung YN, Kim YH, Kim YJ, Park JP, Kwon DK, Kwon OS, Heo JH, Kim YH, Ryu S, Kang HJ, Paek SH, Wang KC, Kim SU, Yoon BW (2009) Effects of human neural stem cell transplantation in canine spinal cord hemisection. Neurol Res 31:996-1002.

Li LM, Han M, Jiang XC, Yin XZ, Chen F, Zhang TY, Ren H, Zhang JW, Hou TJ, Chen Z, Ou-Yang HW, Tabata Y, Shen YQ, Gao JQ (2017) Peptide-tethered hydrogel scaffold promotes recovery from spinal cord transection via synergism with mesenchymal stem cells. ACS Appl Mater Interfaces 9:3330-3342.

Li X, Liu S, Zhao Y, Li J, Ding W, Han S, Chen B, Xiao Z, Dai J (2016) Training neural stem cells on functional collagen scaffolds for severe spinal cord injury repair. Adv Funct Mater 26:5835-5847.

Li X, Fan C, Xiao Z, Zhao Y, Zhang H, Sun J, Zhuang Y, Wu X, Shi J, Chen Y, Dai J (2018) A collagen microchannel scaffold carrying paclitaxel-liposomes induces neuronal differentiation of neural stem cells through Wnt/β-catenin signaling for spinal cord injury repair. Biomaterials 183:114-127.

Liang W, Han Q, Jin W, Xiao Z, Huang J, Ni H, Chen B, Kong J, Wu J, Dai J (2010) The promotion of neurological recovery in the rat spinal cord crushed injury model by collagen-binding BDNF. Biomaterials 31:8634-8641.

Libro R, Bramanti P, Mazzon E (2017) The combined strategy of mesenchymal stem cells and tissue-engineered scaffolds for spinal cord injury regeneration. Exp Ther Med 14:3355-3368.

Liu D, Li X, Xiao Z, Yin W, Zhao Y, Tan J, Chen B, Jiang X, Dai J (2019) Different functional bio-scaffolds share similar neurological mechanism to promote locomotor recovery of canines with complete spinal cord injury. Biomaterials 214:119230.

Lu P, Ceto S, Wang Y, Graham L, Wu D, Kumamaru H, Staufenberg E, Tuszynski MH (2017) Prolonged human neural stem cell maturation supports recovery in injured rodent CNS. J Clin Invest 127:3287-3299.

Lu P, Woodruff G, Wang Y, Graham L, Hunt M, Wu D, Boehle E, Ahmad R, Poplawski G, Brock J, Goldstein LS, Tuszynski MH (2014) Long-distance axonal growth from human induced pluripotent stem cells after spinal cord injury. Neuron 83:789-796.

Lu P, Wang Y, Graham L, McHale K, Gao M, Wu D, Brock J, Blesch A, Rosenzweig ES, Havton LA, Zheng B, Conner JM, Marsala M, Tuszynski MH (2012) Long-distance growth and connectivity of neural stem cells after severe spinal cord injury. Cell 150:1264-1273.

Luo Y, Coskun V, Liang A, Yu J, Cheng L, Ge W, Shi Z, Zhang K, Li C, Cui Y, Lin H, Luo D, Wang J, Lin C, Dai Z, Zhu H, Zhang J, Liu J, Liu H, deVellis J, et al. (2015) Single-cell transcriptome analyses reveal signals to activate dormant neural stem cells. Cell 161:1175-1186.

McCreedy DA, Wilems TS, Xu H, Butts JC, Brown CR, Smith AW, Sakiyama-Elbert SE (2014) Survival, differentiation, and migration of high-purity mouse embryonic stem cell-derived progenitor motor neurons in fibrin scaffolds after sub-acute spinal cord injury. Biomater Sci 2:1672-1682.

Mothe AJ, Tator CH (2013) Review of transplantation of neural stem/progenitor cells for spinal cord injury. Int J Dev Neurosci 31:701-713.

Mukhamedshina YO, Gracheva OA, Mukhutdinova DM, Chelyshev YA, Rizvanov AA (2019) Mesenchymal stem cells and the neuronal microenvironment in the area of spinal cord injury. Neural Regen Res 14:227-237.

Murphy AR, Laslett A, O'Brien CM, Cameron NR (2017) Scaffolds for 3D in vitro culture of neural lineage cells. Acta Biomater 54:1-20.

Nomura H, Tator CH, Shoichet MS (2006) Bioengineered strategies for spinal cord repair. J Neurotrauma 23:496-507.

Ogawa Y, Sawamoto K, Miyata T, Miyao S, Watanabe M, Nakamura M, Bregman BS, Koike M, Uchiyama Y, Toyama Y, Okano H (2002) Transplantation of in vitro-expanded fetal neural progenitor cells results in neurogenesis and functional recovery after spinal cord contusion injury in adult rats. J Neurosci Res 69:925-933.

Raynald, Shu B, Liu XB, Zhou JF, Huang H, Wang JY, Sun XD, Qin C, An YH (2019) Polypyrrole/polylactic acid nanofibrous scaffold cotransplanted with bone marrow stromal cells promotes the functional recovery of spinal cord injury in rats. CNS Neurosci Ther 25:951-964.

Rooney GE, Knight AM, Madigan NN, Gross L, Chen B, Giraldo CV, Seo S, Nesbitt JJ, Dadsetan M, Yaszemski MJ, Windebank AJ (2011) Sustained delivery of dibutyryl cyclic adenosine monophosphate to the transected spinal cord via oligo [(polyethylene glycol) fumarate] hydrogels. Tissue Eng Part A 17:1287-1302.

Saito N, Pulford KA, Breton-Gorius J, Massé JM, Mason DY, Cramer EM (1991) Ultrastructural localization of the CD68 macrophage-associated antigen in human blood neutrophils and monocytes. Am J Pathol 139:1053-1059.

Sakiyama-Elbert S, Johnson PJ, Hodgetts SI, Plant GW, Harvey AR (2012) Scaffolds to promote spinal cord regeneration. Handb Clin Neurol 109:575-594.

Saruhashi Y, Young W, Perkins R (1996) The recovery of 5-HT immunoreactivity in lumbosacral spinal cord and locomotor function after thoracic hemisection. Exp Neurol 139:203-213.

Schoof H, Apel J, Heschel I, Rau G (2001) Control of pore structure and size in freeze-dried collagen sponges. J Biomed Mater Res 58:352-357.

Shrestha B, Coykendall K, Li Y, Moon A, Priyadarshani P, Yao L (2014) Repair of injured spinal cord using biomaterial scaffolds and stem cells. Stem Cell Res Ther 5:91.

Sun Y, Yang C, Zhu X, Wang JJ, Liu XY, Yang XP, An XW, Liang J, Dong HJ, Jiang W, Chen C, Wang ZG, Sun HT, Tu Y, Zhang S, Chen F, Li XH (2019) 3D printing collagen/chitosan scaffold ameliorated axon regeneration and neurological recovery after spinal cord injury. J Biomed Mater Res A 107:1898-1908.

Teng YD, Lavik EB, Qu X, Park KI, Ourednik J, Zurakowski D, Langer R, Snyder EY (2002) Functional recovery following traumatic spinal cord injury mediated by a unique polymer scaffold seeded with neural stem cells. Proc Natl Acad Sci U S A 99:3024-3029.

Thuret S, Moon LD, Gage FH (2006) Therapeutic interventions after spinal cord injury. Nat Rev Neurosci 7:628-643.

Wang Z, Long DW, Huang Y, Chen WCW, Kim K, Wang Y (2019) Decellularized neonatal cardiac extracellular matrix prevents widespread ventricular remodeling in adult mammals after myocardial infarction. Acta Biomater 87:140-151.

Xu B, Zhao Y, Xiao Z, Wang B, Liang H, Li X, Fang Y, Han S, Li X, Fan C, Dai J (2017) A dual functional scaffold tethered with EGFR antibody promotes neural stem cell retention and neuronal differentiation for spinal cord injury repair. Adv Healthc Mater 6:1601279.

Yan Q, Ruan JW, Ding Y, Li WJ, Li Y, Zeng YS (2011) Electro-acupuncture promotes differentiation of mesenchymal stem cells, regeneration of nerve fibers and partial functional recovery after spinal cord injury. Exp Toxicol Pathol 63:151-156.

Yoshii S, Oka M, Shima M, Taniguchi A, Taki Y, Akagi M (2004) Restoration of function after spinal cord transection using a collagen bridge. J Biomed Mater Res A 70:569-575.

Yuan T, Liu Q, Kang J, Gao H, Gui S (2019) High-dose neural stem/progenitor cell transplantation increases engraftment and neuronal distribution and promotes functional recovery in rats after acutely severe spinal cord injury. Stem Cells Int 2019:9807978.

P-Reviewers: Fischer I, Litofsky NS; C-Editor: Zhao M; S-Editors: Yu J, Li CH; L-Editors: Patel B, Yu J, Song LP; T-Editor: Jia Y

Additional Table 1 Basso, Beattie and Bresnahan locomotor rating scale

Score	Feature
0	No observable hindlimb (HL) movement
1	Slight movement of one or two joints, usually the hip and/or knee
2	Extensive movement of one joint or extensive movement of one joint and slight movement of one other joint
3	Extensive movement of two joints
4	Slight movement of all three joints of the HL
5	Slight movement of two joints and extensive movement of the third
6	Extensive movement of two joints and slight movement of the third
7	Extensive movement of all three joints of the HL
8	Sweeping with no weight support or plantar placement of the paw with no weight support
9	Plantar placement of the paw with weight support in stance only (i.e., when stationary) or occasional, frequent, or consistent weight-supported dorsal stepping and no plantar stepping
10	Occasional weight-supported plantar steps; no forelimb (FL)–HL coordination
11	Frequent to consistent weight-supported plantar steps and no FL–HL coordination
12	Frequent to consistent weight-supported plantar steps and occasional FL–HL coordination
13	Frequent to consistent weight-supported plantar steps and frequent FL–HL coordination
14	Consistent weight-supported plantar steps, consistent FL–HL coordination, and predominant paw position during locomotion is rotated (internally or externally) when it makes initial contact with the surface as well as just before it is lifted off at the end of stance; or frequent plantar stepping, consistent FL–HL coordination, and occasional dorsal stepping
15	Consistent plantar stepping and consistent FL–HL coordination and no toe clearance or occasional toe clearance during forward limb advancement; predominant paw position is parallel to the body at initial contact
16	Consistent plantar stepping and consistent FL–HL coordination during gait and toe clearance occurs frequently during forward limb advancement; predominant paw position is parallel at initial contact and rotated at lift off
17	Consistent plantar stepping and consistent FL–HL coordination during gait and toe clearance occurs frequently during forward limb advancement; predominant paw position is parallel at initial contact and lift off
18	Consistent plantar stepping and consistent FL–HL coordination during gait and toe clearance occurs consistently during forward limb advancement; predominant paw position is parallel at initial contact and rotated at lift off
19	Consistent plantar stepping and consistent FL–HL coordination during gait, toe clearance occurs consistently during forward limb advancement, predominant paw position is parallel at initial contact and lift off, and tail is down part or all of the time
20	Consistent plantar stepping and consistent coordinated gait, consistent toe clearance, predominant paw position is parallel at initial contact and lift off, and trunk instability; tail consistently up
21	Consistent plantar stepping and coordinated gait, consistent toe clearance, predominant paw position is parallel throughout stance, and consistent trunk stability; tail consistently up

Slight: partial joint movement through less than half the range of joint motion; Extensive: movement through more than half of the range of joint motion; Sweeping: rhythmic movement of HL in which all three joints are extended, then fully flex and extend again; animal is usually sidelying, the plantar surface of paw may or may not contact the ground; no weight support across the HL is evident; No Weight Support: no contraction of the extensor muscles of the HL during plantar placement of the paw; or no elevation of the hindquarter; Weight Support: contraction of the extensor muscles of the HL during plantar placement of the paw, or elevation of the hindquarter; Plantar Stepping: The paw is in plantar contact with weight support then the HL is advanced forward and plantar contact with weight support is reestablished; Dorsal Stepping: weight is supported through the dorsal surface of the paw at some point in the step cycle; FL-HL Coordination: for every FL step an HL step is taken and the HLs alternate; Occasional: less than or equal to half; < 50%; Frequent: more than half but not always; 51-94%; Consistent: nearly always or always; 95-100%.

Additional Table 2 Porosity (%) of collagen scaffold with axially-aligned luminal conduits

Scaffold	Porosity
Sample 1	85.51
Sample 2	87.75
Sample 3	84.96
Sample 4	85.24